

Dopant Sources Choice for Formation of *p*-Type ZnO: Phosphorus Compound Sources

Zhi Gen Yu,^{†,‡} Hao Gong,[‡] and Ping Wu^{*,†}

*Institute of High Performance Computing, 1 Science Park Road,
#01-01 The Capricorn, Singapore 117528, and Department of Materials Science, National University of
Singapore, 10 Kent Ridge Crescent, Singapore 119260*

Received October 12, 2004. Revised Manuscript Received December 7, 2004

Fabrication of *p*-type ZnO has proven difficult and usually inconsistent despite numerous worldwide efforts. In this theoretical study we explored the problem of *p*-type ZnO formation using both DFT and thermochemistry calculations. Our DFT models predicted that Zn₃P₂ is a good dopant because it can lead to a shallow acceptor level at 0 K. Additional thermochemistry calculations demonstrated that this shallow acceptor can be further stabilized in a real fabrication process. Our models explain well the observed trends for both *n*- and *p*-type phosphorus-doped ZnO and especially the observed inconsistent behaviors of P₂O₅ dopant. A new strategy of fabricating *p*-type ZnO was proposed thereafter. This research may also help to address the problem of dopant selection in the fabrication of other wide-gap semiconductors.

Introduction

Fabrication of optoelectronic devices such as blue and UV lasers and light emitting diodes (LEDs) is one of the most attractive applications of wide-gap semiconductors. However, unlike the silicon technology it is very difficult to make a *p*–*n* homojunction using wide-gap semiconductors. They either form *n*-type or *p*-type but not both types; ZnO and CuAlSe₂ are respectively good *n*-type and *p*-type semiconductors, but not vice versa.¹ A *p*–*n* homojunction using a wide-gap semiconductor has wide applications including the functional window to transmit visible light and generate electricity in response to the absorption of UV photons.² Many studies have been reported recently^{3–11} to fabricate usable *p*-type ZnO and of special interest is the codoping method proposed by Yamamoto and Hiroshi¹² and further developed by others.^{13–15} It was found that by applying

different forms of dopant sources which contain the same dopant chemical element might result in different types (*n*- or *p*-) of semiconductors. For instance, using N₂ as the dopant source led to *n*-type conduction³ but NO₂ or NO led to *p*-type conduction;^{4,5} using P₂O₅ led to *n*-type conduction⁹ (poor reproducible *p*-type conduction⁷ also was reported) but Zn₃P₂ led to *p*-type conduction experimentally.^{6,8} Some DFT calculations^{16–18} were reported focusing on relationships between oxygen chemical potential and electronic band gap structure, since the difference in oxygen chemical potential may be partially responsible for the above ZnO experiments. However, the underline mechanism that governs the above observed dopant behavior is still not clear. In this paper, we report the electronic band gap structures of P-doped ZnO under different growth conditions using various dopant sources. We further explore this problem from both DFT and chemical thermodynamic calculations. Our results indicate that it is unlikely to fabricate a usable *p*-type ZnO using P₂O₅ as dopant. On the other hand, we predicted that Zn₃P₂ is a good dopant source under zinc rich growth conditions. We also propose a systematic and scientific method on how to choose dopant source for P-doped ZnO.

Methodology

First principles DFT calculations were performed by using the Kohn–Sham DFT^{19,20} within the generalized gradient approximation (GGA).²¹ The plane-wave total energy method²² as imple-

* Corresponding author. E-mail: wuping@ihpc.a-star.edu.sg. Telephone: (65) 6419-1212. Fax: (65) 6778 0522.

[†] Institute of High Performance Computing.

[‡] National University of Singapore.

- (1) Zhang, S. B.; Wei S.-H.; Zunger, A. *J. Appl. Phys.* **1998**, *83*, 3192.
- (2) Kawazoe, H.; et al. *Nature* **1997**, *389*, 939.
- (3) Li, X.; et al., *Electrochem. Solid State Lett.* **2003**, *6*, c56.
- (4) Guo, X.-L.; Tabata, H.; Kawai, T. *Opt. Mater.* **2002**, *19*, 229. Guo, X.-L.; Tabata, H.; Kawai, T. *J. Cryst. Growth* **2001**, *223*, 135.
- (5) Li, X.; et al. *J. Vac. Sci. Technol. A* **2003**, *21*, 1342.
- (6) Aoki, T.; Hatanaka, Y.; Look, D. C. *Appl. Phys. Lett.* **2000**, *76*, 3257.
- (7) Kim, K.-K.; Kim, H.-S.; Hwang, D.-K.; Lim, J.-H.; Park, S.-J. *Appl. Phys. Lett.* **2003**, *83*, 63.
- (8) Bang, K.-H.; et al. *Appl. Surf. Sci.* **2003**, *210*, 177.
- (9) Heo, Y. W.; et al. *Appl. Phys. Lett.* **2003**, *83*, 1128. Heo, Y. W.; et al. *Appl. Phys. A* **2004**, *78*, 53.
- (10) Tsukazaki, A.; et al. *Appl. Phys. Lett.* **2002**, *81*, 235.
- (11) Sanmyo, M.; Tomita, Y.; Kobayashi, K. *Chem. Mater.* **2003**, *15*, 819.
- (12) Yamamoto, T.; Hiroshi, K.-Y. *Jpn. J. Appl. Phys.* **1999**, *38*, L166–L169.
- (13) Ohshima, T.; Ikegami, T.; Ebihara, K.; Asmussen, J.; Thareja, R. *Thin Solid Films* **2003**, *435*, 49.
- (14) Wang, L. G.; Zunger A. *Phys Rev B* **2003**, *68*, 125211.
- (15) Bian, J. M.; Li, X. M.; Chen, L. D.; Yao, Q. *Chem. Phys. Lett.* **2004**, *293*, 256.

- (16) Oba, F.; Nishitani, S. N.; Isotani, S.; Adachi, H. *J. Appl. Phys.* **2001**, *90*, 824.
- (17) Zhang, S. B.; Wei, S.-H.; Zunger, A. *Phys. Rev. B* **2001**, *63*, 075205.
- (18) Lee, E.-C.; Kim, Y.-S.; Jin, Y.-G.; Chang, K. J. *Phys. Rev. B* **2001**, *64*, 085120. Lee, E.-C.; Kim, Y.-S.; Jin, Y.-G.; Chang, K. J. *Physica B* **2001**, *308–310*, 912.
- (19) Kohn, W.; Sham, L. J. *Phys. Rev.* **1965**, *140*, A1133.
- (20) Jones, R. O.; Gunnarsson, O. *Rev. Mod. Phys.* **1989**, *61*, 689.
- (21) Perdew, J. P.; et al. *Phys. Rev. B* **1992**, *46*, 6671.
- (22) Ihm, J.; Zunger, A.; Cohen, M. L. *J. Phys. C* **1979**, *12*, 4409.

mented in the CASTEP code^{23,24} was employed. The self-consistent total energy in the ground state was effectively obtained by the density-mixed scheme.²⁵ Atomic positions were optimized by minimizing the total energy using the quasi-Newton method with the Broyden–Fletcher–Goldfarb–Shanno Hessian update scheme (BFGS).²⁶ Ultrasoft pseudopotentials^{27,28} were employed to treat “shallow” core electrons as valence states by including multiple sets of occupied states in each angular momentum channel. This leads to high accuracy and transferability of the potentials. The next uppermost states of O (2s, 2p), P (3s, 3p) and Zn (3d, 4s) were explicitly treated as parts of the valence states, respectively. 72-Atom wurtzite supercells doped with one P atom were adopted in the calculation and a 108-atom supercell was also used to test the convergence. Because of the large size of the supercell, only one k point is necessary for k -space integrations. Selecting the Γ point, we find that the total energy is converged within 5 meV/ZnO for defects. A plane-wave cutoff energy of 400 eV was chosen, relaxing all atoms and leaving the lattice constants frozen until the SCF convergence per atom was below 2×10^{-5} eV.

Energies of Doped P Formation

In this work, two possible positions (interstitial and substitutional) of P in ZnO were taken into account. The formation energy of an interstitial P can be written as

$$E_f^q = (E_{def}^q - E_{per,0}^0) - \mu_P + qE_e \quad (1)$$

and the formation energy of a substitutional P at O and Zn sites can be expressed respectively, by

$$E_f^q = (E_{def}^q - E_{per,0}^0) - (\mu_P - \mu_O) + qE_e \quad (2)$$

and

$$E_f^q = (E_{def}^q - E_{per,0}^0) - (\mu_P - \mu_{Zn}) + qE_e \quad (3)$$

where E_{def}^q is the total energy of the supercell with a doped P in the charged state q , $E_{per,0}^0$ is the total energy of the perfect supercell, and $\mu_{P,Zn,O}$ denotes the corresponding atomic chemical potential. E_e is the Fermi energy of ZnO. Normally, the Fermi level is considered to vary between the valence band and the conduction band. Due to the severe underestimation of the band gap by using DFT calculations, as a standard practice the Fermi energy is chosen to correspond to the experimental band gap value rather than the theoretical one without effect on the computational ionization level.²⁹

When charged systems were studied, a uniform charge neutralizing background was applied. This approach leads to an error due to the electrostatic interactions between the charge and its images which was corrected by using Madelung energy.^{30,31}

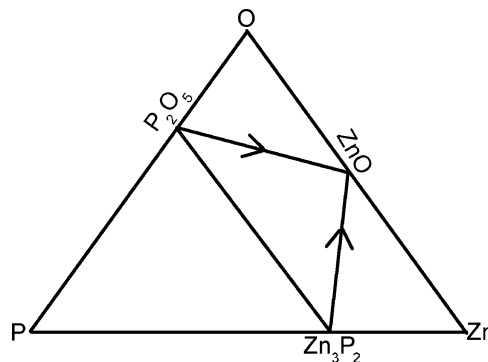


Figure 1. Doping paths in Zn–O–P ternary system.

For ZnO, the chemical potential of oxygen (zinc) μ_{O}^{ZnO} (μ_{Zn}^{ZnO}) varies between $\mu_O^0 + \Delta E_f^{ZnO}(\mu_{Zn}^0)$ and μ_O^0 ($\mu_{Zn}^0 + \Delta E_f^{ZnO}$),²⁹ corresponding to the limiting growth conditions of oxygen poor (zinc rich) and oxygen rich (zinc poor) were used to analyze the effect on the formation energy of doped P. The total energies of per atom for molecule oxygen and bulk zinc ($P6_3/mmc$) were chosen as the upper limits of chemical potential of oxygen (μ_O^0) and zinc (μ_{Zn}^0), respectively. ΔE_f^{ZnO} is the heat of the formation of ZnO, which was calculated to be 3.94 eV/ZnO. This value is close to the experimental value of 3.63 eV.³²

Fabrication of P-doped ZnO may be carried out under a range of oxygen, zinc, and phosphorus partial pressures. According to eqs 1–3, assuming chemical equilibrium, these partial pressures affect the formation energy of P in ZnO. In a Zn–O–P ternary system at ~ 400 °C (which represents the fabrication temperature) as shown in Figure 1, phosphorus doping in ZnO can be carried out either along the ZnO– P_2O_5 or the ZnO– Zn_3P_2 binary, the P–ZnO binary is not stable which either belongs to the ZnO– P_2O_5 – Zn_3P_2 or the P– P_2O_5 – Zn_3P_2 ternary depends on the phosphorus concentration. Hence, we focus on the ZnO– P_2O_5 – Zn_3P_2 system and only study the dopant behaviors of P_2O_5 (under both oxygen rich and oxygen poor) and of Zn_3P_2 (under zinc rich and zinc poor growth conditions).

In the P_2O_5 –ZnO system, we have

$$5\mu_O^{P_2O_5} + 2\mu_P^{P_2O_5} = \mu_{P_2O_5}^{bulk} \quad (4)$$

where $\mu_P^{P_2O_5}$, $\mu_O^{P_2O_5}$, and $\mu_{P_2O_5}^{bulk}$ are the chemical potential of P, O, and P_2O_5 . The total energy of per unit formula of P_2O_5 with phosphorus pentoxide orthorhombic tetramolecular unit cell ($Pnma$)³³ was calculated as $\mu_{P_2O_5}^{bulk}$. The computed lattice parameters are $a = 9.35$ Å (9.23 Å), $b = 4.88$ Å (4.94 Å), and $c = 7.21$ Å (7.18 Å); the values in parentheses are the experimental values from ref 33. The effect of oxygen partial pressure on the fabrication of P-doped ZnO was investigated by taking $\mu_O^{P_2O_5}$ from $\mu_O^0 + \mu_O^{P_2O_5}$ (oxygen poor) and μ_O^0

(23) Payne, M. C.; et al. *Rev. Mod. Phys.* **1992**, *64*, 1050.

(24) Milman, V.; et al. *Int. J. Quantum Chem.* **2000**, *77*, 895.

(25) Kresse, G.; Furthmüller, J. *Phys. Rev. B* **1996**, *54*, 11169.

(26) Press, W. H.; Teukolsky, S. A.; Vetterling, W. T.; Flannery, B. P. *Numerical Recipes in FORTRAN: The Art of Scientific Computing*, 2nd ed.; Cambridge University Press: Cambridge, 1992; p 418.

(27) Vanderbilt, D. *Phys. Rev. B* **1990**, *41*, 7892.

(28) Laasonen, K.; Car, R.; Lee, C.; Vanderbilt, D. *Phys. Rev. B* **1991**, *43*, 6796.

(29) Zhi, G. Y.; Hao, G.; Ping, W. Unpublished. Kohan, A. F.; Ceder, G.; Morgan, D.; Van de Walle, C. G. *Phys. Rev. B* **2000**, *61*, 15019.

(30) Makov, G.; Payne, M. C. *Phys. Rev. B* **1995**, *51*, 4014.

(31) Lento, J.; Mozos J.-L.; Nieminen, R. M. *J. Phys.: Condens. Matter* **2002**, *14*, 2637.

(32) Cox, J. D.; Wagman, D. D.; Medvedev, V. A. *CODATA key values for thermodynamics*; Hemisphere: New York, 1989; p 48.

(33) Wyckoff, R. W. *Crystal Structures*, 2nd ed.; Robert E. Krieger Publishing Co.: Malabar, FL, 1986; Vol. 1, p 184.

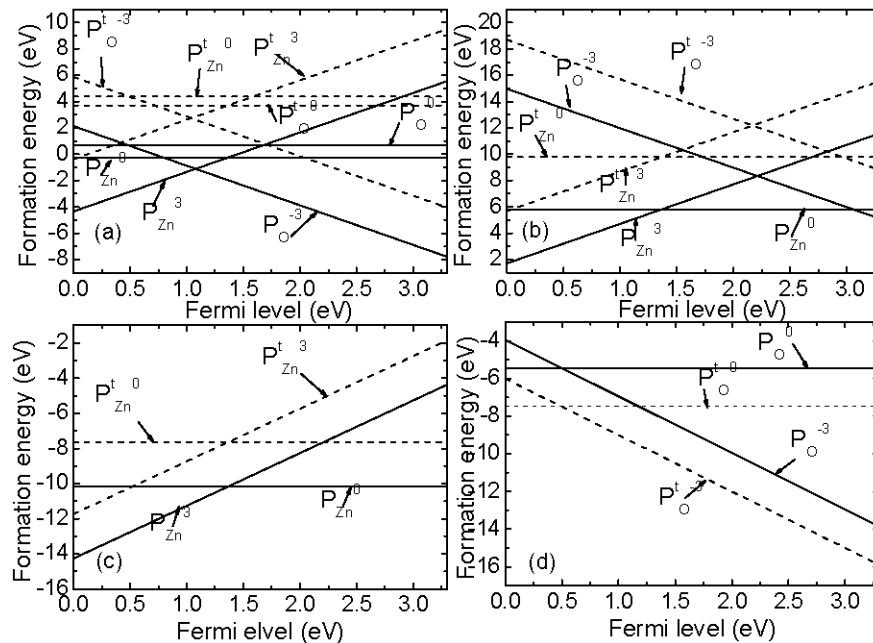


Figure 2. Formation energies of doped P in ZnO. (a, b) ZnO–P₂O₅ system under oxygen poor and rich conditions, respectively; (c, d) ZnO–Zn₃P₂ system under zinc poor and rich conditions, respectively. The solid lines denote the DFT computing results at 0 K, and the dashed lines denote the thermochemistry computing results (In ZnO–P₂O₅ system, the temperature is set at 358 °C; in ZnO–Zn₃P₂ system, the temperature is set at 400 °C). Here, P_x^t and P_xⁱ denote the substitutional P of X site (X for Zn or O) at 0 K and the elevated temperature, respectively.

(oxygen rich), and the results are shown in Figure 2a and b, respectively.

Similarly in the Zn₃P₂–ZnO system, we have

$$3\mu_{\text{Zn}}^{\text{Zn}_3\text{P}_2} + 2\mu_{\text{P}}^{\text{Zn}_3\text{P}_2} = \mu_{\text{Zn}_3\text{P}_2}^{\text{bulk}} \quad (5)$$

where $\mu_{\text{P}}^{\text{Zn}_3\text{P}_2}$, $\mu_{\text{Zn}}^{\text{Zn}_3\text{P}_2}$, and $\mu_{\text{Zn}_3\text{P}_2}^{\text{bulk}}$ are the chemical potentials of P, Zn, and Zn₃P₂. The total energy of per unit formula of Zn₃P₂ with zinc phosphate unit cell (P4₂/nmc)³³ was calculated as $\mu_{\text{Zn}_3\text{P}_2}^{\text{bulk}}$. The computed lattice parameters are $a = b = 8.04$ Å (8.09 Å) and $c = 11.38$ Å (11.41 Å); the values in parentheses are the experimental values from ref 33. The effect of zinc partial pressure on the fabrication of P-doped ZnO was investigated by varying $\mu_{\text{Zn}}^{\text{Zn}_3\text{P}_2}$ from $\mu_{\text{Zn}}^0 + \Delta E_f^{\text{ZnO}}$ (zinc poor) to μ_{Zn}^0 (zinc rich), and the results are shown in Figure 2c and d, respectively.

Results and Discussion

The temperature factor was not included in the above DFT calculations which assume 0 K. To estimate the thermal effects of a real fabrication process, chemical thermodynamic calculations were performed. Assuming the gas phase is in chemical equilibrium with the ZnO thin film, chemical potential of P in eq 1, chemical potential difference between P and O in eq 2, and between P and Zn in eq 3 equal, respectively, to that of P, P–O, and P–Zn in the gas phase.

A commercial thermochemistry software, FACTSage,³⁴ was used to calculate respectively the phase equilibrium in the (ZnO + P₂O₅) and the (ZnO + Zn₃P₂) mixtures from room temperature to ~400 °C. The results are shown in Table 1. It is seen that μ_{P} , ($\mu_{\text{P}} - \mu_{\text{O}}$) and ($\mu_{\text{P}} - \mu_{\text{Zn}}$) shift negatively relevant to those of 0 K, except ($\mu_{\text{P}} - \mu_{\text{O}}$) from

Table 1. Changes of the Chemical Potentials of Relevant Elements Relative to 0 K Using Thermochemistry Calculations

dopant source	<i>T</i> (°C)	μ_{P} (eV)	$\mu_{\text{P}} - \mu_{\text{O}}$ (eV)	$\mu_{\text{P}} - \mu_{\text{Zn}}$ (eV)
P ₂ O ₅	250	−6.87	−3.72	−3.97
	300	−6.60	−3.72	−3.96
	350	−6.72	−3.72	−3.96
	358	−6.71	−3.72	−3.96
	400	−6.71	−3.72	−3.96
Zn ₃ P ₂	250	−3.06	2.04	−2.53
	300	−3.06	2.04	−2.53
	350	−3.06	2.04	−2.53
	358	−3.06	2.04	−2.53
	400	−3.06	2.04	−2.53

Zn₃P₂. It is also found that these values change little in the range of the list temperature. By inserting the chemical potential data in Table 1 into eqs 1–3, modifications due to a thermal effect were estimated as shown in Figure 2a–d (dashed lines).

It is our interest to study the formation mechanism of P-doped centers in ZnO by exploring the above results. Figure 2 shows formation energies of various possible charged states of doped P in ZnO as a function of the Fermi level within the measured forbidden gap. Each line in Figure 2 corresponds to a specific charged state of the doped P, and the slope of each line corresponds to the charge of that doped P (see eqs 1–3). An intersection of two lines in Figure 2 corresponds to transition energy (level) of two charged states. All possible charged states of doped P including substitutional and interstitial are calculated and only these with the lower end of formation energy are plotted in Figure 2. Our main findings are showed below:

(i) P-Doped ZnO using P₂O₅ as the dopant under oxygen poor condition leads to unstable *p*-type conduction. In Figure 2a, a shallow acceptor locates at 0.49 eV above the top of valence band, and (or) a deep donor forms at ~1.36 eV above the top of valence band. The acceptor would be in dominant state if the substitutional P of zinc site is suppressed.

However, the formation energy of P_{Zn}^3 is lower than that of P_O^{-3} . So that it is the dominant state. Hence, the deep donor which is more stable than the acceptor would dilute hole-concentration which makes the *p*-type conduction unstable. A thermal effect is not expected to improve the situation at all, since these values do not vary much. However, as long as the deep donor is inhibited by any means, *p*-type conduction is possible.

(ii) P-Doped ZnO using P_2O_5 as the dopant under oxygen rich condition leads to *n*-type conduction. In Figure 2b, a shallow donor which is ~ 1.37 eV above the top of valence band appears in P-doped ZnO, and remains stable at elevated temperatures. We also found a deep acceptor (P_O^{-3}) at ~ 3 eV above the top of valence band. Hence, in this doping system, *n*-type ZnO is obtained. The model prediction is supported by the experimental observation of ref 9 which showed P-doped ZnO exhibits good *n*-type condition.

(iii) P-Doped ZnO using Zn_3P_2 as the dopant under zinc poor condition does not show *p*-type conduction. In Figure 2c only deep donors exist under this growth condition at all temperatures. The dominant states are substitutional P with charged states of +3 or neutral. Experiments under these growth conditions are expected to produce no *p*-type conduction at all.

(iv) P-Doped ZnO using Zn_3P_2 as the dopant under zinc rich condition leads to good *p*-type conduction. In Figure 2d a very shallow acceptor at ~ 0.47 eV above the top of

the valence band appears under this growth condition at high temperatures. The formation energies of donor (P_{Zn}^q) move up and the formation energies of acceptor (P_O^q) move down. The thermal effect becomes the winning factor for the shallow acceptor. Lower formation energy would ensure high solubility as well as higher carrier concentration. The *p*-type conductivity is therefore becoming more stable and stronger at an elevated temperature. P_O^q has lower formation energy and still remains in the dominant state competing with the oxygen vacancy.²⁹ Our model prediction is supported by the experiments⁶⁻⁹ which indicated that Zn_3P_2 is a better dopant source than P_2O_5 . We recommend the use of Zn_3P_2 dopant and zinc rich growth condition in the fabrication of *p*-type ZnO.

Conclusions

We calculate the formation energies of all possible charged states of doped P from two candidate dopant sources. We find that Zn_3P_2 is a better dopant source than P_2O_5 , especially at an elevated temperature. The same approach used in this study may be applied to the design of dopant source as well as the growth conditions for other wide-gap semiconductors.

Acknowledgment. The authors thank R. M. Nieminen of HUT, Finland, for his helpful advice on Madelung energy correction. This work was supported by A*STAR of Singapore.

CM0482176